International Journal of Machine Tools and Manufacture, Volume 65, February 2013, Pages 15–21

Brittle-ductile transition during diamond turning of single crystal silicon carbide

Saurav Goel[ab], Xichun Luo[ab]*, Paul Comley[c], Robert L Reuben[a] and Andrew Cox[d]

[a]School of Engineering and Physical Sciences, Heriot-Watt University, Edinburgh, EH144AS, Scotland, UK

[b]School of Computing and Engineering, University of Huddersfield, Huddersfield HD13DH,UK

[c]School of Applied Sciences, Cranfield University, Cranfield, Bedfordshire, MK430AL, UK

[d] Contour Fine Tooling, Wedgwood Court, Stevenage, Hertfordshire, SG14QR, UK

*Corresponding author Tel.: +44 1484 473806, Email address: x.luo@hud.ac.uk, Fax: +44 1484 472161

Abstract:

In this experimental study, diamond turning of single crystal 6H-SiC was performed at a cutting speed of 1 m/sec on an ultra precision diamond turning machine (Moore Nanotech 350 UPL) to elucidate the microscopic origin of ductile-regime machining. Distilled water (pH value 7) was used as a preferred coolant during the course of machining in order to improve the tribological performance. A high magnification scanning electron microscope (SEM) (FIB- FEI Quanta 3D FEG) was used to examine the cutting tool. A surface finish of Ra 9.2 nm, better than any previously reported value on SiC was obtained. Also, tremendously high cutting resistance was offered by SiC resulting in the observation of significant wear marks on the cutting tool just after 1 Km of cutting length. It was found out through a DXR Raman microscope that similar to other classical brittle materials (silicon and germanium etc.) an occurrence of brittle-ductile transition is responsible for the ductile-regime machining of 6H-SiC. It has also been demonstrated that the structural phase transformations associated with the diamond turning of brittle materials which is normally considered as a prerequisite to ductile-regime machining, may not well be realized during machining of polycrystalline materials, yet, ductile-regime exploitation is possible.

Keywords: silicon carbide; diamond turning; brittle-ductile transition.

Abbreviations:

3C-SiC	3C type silicon carbide
6H-SiC	6H type silicon carbide
BDT	Brittle-ductile transition
CBN	Cubic boron nitride
CIS	Critical indent size
CVD-SiC	Chemically vapour deposited silicon carbide
FIB	Focussed ion beam
RB-SiC	Reaction-bonded silicon carbide
SEM	Scanning electron microscope
SPDT	Single point diamond turning
UPL	Ultra precision lathe

Nomenclatures:

dc	Critical chip thickness
E	Elastic modulus of the material
f_{max}	Critical feed rate
H	Hardness
K_c	Fracture toughness
N	Spindle speed
R	Nose radius of the cutting tool
t_{max}	Maximum critical chip thickness
V	Cutting speed
Yc	Critical crack length

1. Introduction

Silicon carbide (SiC) is an ultra hard ceramic material possessing desirable engineering properties such as chemical inertness, high thermal conductivity, high carrier saturation velocity, high specific stiffness (E/ρ) and high-temperature resistance [1]. For these reasons, SiC is an appropriate choice for the purpose of quantum computing applications as a substitute to diamond [2], in space based laser mirrors [3-4] and for molding dies used for hot-press molding of aspherical glass lenses. However, the extreme high micro-hardness of SiC makes it a difficult to machine material even with the hardest known, diamond cutting tool [5].

Single point diamond turning (SPDT) is an established ultra precision manufacturing method used to produce an optics in a single machining pass with the aid of a single point diamond cutting tool [6]. SPDT is preferred for its unique capabilities to efficiently produce three dimensional freeform structures. Moreover, the components produced through an SPDT operation possess a much better metallurgical structure than the one obtained through polishing and lapping processes [7]. This compounds further with the fact that SPDT offers flexibility of generated figure, better step-definition, deterministic form accuracy and economy of fabrication time [8]. Therefore, SPDT of silicon carbide (SiC) is of significant technological interest and economic advantage for various industrial applications [9-10]. The aim of this work is to principally investigate the microscopic origin of ductile-regime machining of 6H-SiC and demonstrate the attainable surface roughness on this ceramic for the purpose of producing optical surface. In general, the attainable surface finish (*Ra*) on the materials shall be within 20 nm in order to qualify as a good optical candidate [5].

2. Literature review

Brittle materials in general, including SiC, exhibit low fracture toughness (CVD 3C-SiC being exception) and are therefore difficult to machine. It is however possible to machine such brittle materials similar to metal-machining at a relatively smaller length scale using appropriate machining parameters. Execution of such kind of machining process on brittle materials where the chips are generated through a mode of plastic deformation rather than fracture is called as ductile-

regime machining. The possibility of machining brittle materials in the so called ductile-regime was first observed by King and Tabor [11] in the year 1954 during frictional wear of rock salts. They realized that although there were some cracks and surface fragmentations, there was some plastic deformation involved. Similarly, Bridgman *et al.* [12] recognized that a brittle material such as glass exhibited ductility under high hydrostatic pressure. Subsequently, Lawn and Wilshaw [13] observed the same ductile behaviour of glass during the nano-indentation testing which lead to the identification of elastic-plastic transition. They realized that the ductile behaviour causes the material to expand in a radial core (hydrostatic core) which exerts a uniform hydrostatic pressure on its surroundings. This radial core is encased within an intermediate core of "plastic region" that is surrounded by a region called "elastic matrix". This observation leads to the identification of elastic-plastic response of brittle materials during their nano-indentation. It was realized during this time that under the influence of large hydrostatic stress almost any material including diamond can be deformed plastically even at low temperatures [14]. In the subsequent work, Lawn and Marshall [15] proposed an empirical relation for the required lower bound of the critical load P and the resulting critical crack length c in the substrate material which they correlated with the fracture toughness and hardness of the substrate material:

$$P = \lambda_0 \left[\frac{K_c^{\,4}}{H^3} \right] \tag{1}$$

$$c = \mu_0 \left[\frac{K_c^{\,2}}{H^2} \right] \tag{2}$$

where λ_0 and μ_0 are the geometrical constants dependent on the material, P is the critical load, c is the crack length, K_c is the fracture toughness which is the resistance to fracture and H is the hardness of the material which was defined as the resistance to the plastic flow. Further development lead to the identification of the critical indent size (CIS) [16] as follows:

$$CIS = \mu \left[\frac{K_c}{H} \right]^2 \qquad \text{where } \mu \propto E/H \text{ and E being the elastic modulus of the material} \tag{3}$$

Subsequently, Bifano *et al.* [17] postulated that each material will be apt to undergo a brittle-ductile transition when subjected to a small infeed rate. Within this small in-feed rate the energy required to propagate a crack is larger than the energy required for plastic yielding, so plastic deformation will become dominant. It was as late as 1990 when Blake and Scattergood [18] suggested that despite the dynamic and geometric differences in material removal mechanism during nano-scratching and a nano-indentation process, there are essential similarities in both these processes. They identified that a critical chip thickness d_c separates the portion of plastic deformation from fracture removal. Accordingly, they proposed a new machining model to explain the ductile regime machining of brittle materials. As per their machining model, a material possessing minimum crack length is preferable in order to avoid the penetration of the crack underneath the machined surface during the course of machining. Usually, the estimation of the various geometrical parameters of this model is about 50% off the actual experimental value [19]. This is due to the unaccountability of the associated structural transformations and associated volume changes (~20%) of the cutting chips in their machining model [20]. However, this model is still quite relevant to relate theoretical understanding with the experimental outcome [21]. An evaluation of the critical parameters such as critical crack length and critical chip thickness of 6H-SiC are shown in table 1. These calculations are based on the empirically known relations as shown earlier.

Table 1: Critical properties of 6H-SiC

S.NO.	Material properties	Unit of measurement	Values
	Fracture Toughness (K_c)	MPa.m$^{1/2}$	1.9
	Hardness (H)	GPa	22
	Elastic Modulus (E)	GPa	347.01
1	Critical Crack Length $Y_c = 120\frac{K_c^{\,2}}{H^2}$	µm	0.895
2	Critical Chip Thickness $d_c = 0.15 \times \frac{E}{H} \times \left(\frac{K_c}{H}\right)^2$	µm	0.01764

With this brief but essential background, initial SPDT trials performed till date on SiC were mainly concerned to study its technical feasibility. These works are tabulated in table 2 highlighting their experimental outcome, type of work material used and the coolant used in those investigations.

Table 2: Experimental trials reported so far on nanometric cutting of SiC.

S.No.	Work Material	Reference Study	Experimental outcome	Coolant used
1.	RB-SiC	Yan *et al.* [22]	Ra : 23 nm	Dry cutting
2.	RB-SiC	Yan *et al.* [23]	Ra: 20 nm; Rz: 400 nm Ra: 14 nm; Rz: 300 nm	Grease of MoS_2 nanoparticles Grease of Cu nanoparticles
3.	3C-CVD SiC	Ravindra *et al.* [10]	Ra: 83 nm and Rz: 530 nm against as received Ra: 1.158 µm & Rz : 8.486 µm.	Masterpolish 2 Final polishing suspension (contains alumina and colloidal silica with a pH~9)
4.	6H-SiC	Patten *et al.* [4, 9, 24]	Ra : Not specified	Dry cutting
5	6H-SiC	Jacob *et al.* [25]	Only a scratching test was performed to establish DBT depth which was found to be about 70 nm for 6H-SiC	
6	4H-SiC	Ravindra *et al.* [5]	Only a scratching test was performed to establish DBT depth which was found to be about 820 nm for 4H-SiC	
7	4H-SiC	Shayan *et al.*[26]	Laser assisted nano-scratching was done to observe the improvement in the machinability of SiC.	

Table 2 suggests that SPDT succeeded to generate a very fine machined surface of Ra value 14 nm

on RB-SiC using copper nanoparticles as a coolant. An inferior Ra value of 23 nm was however obtained on the same RB-SiC while dry cutting. Similarly, 3C type polycrystalline CVD-SiC was machined upto an Ra value of 83 nm against as received Ra value of 1.158 μm using an alumina and silica based specialized coolant.

Surprisingly, no surface roughness data has been reported on single crystal SiC despite the fact that there are significant differences in the nature of bonding, microstructure, extent of plastic deformation, number of slip systems between single crystal and polycrystalline SiC. Although, polycrystalline SiC is relatively easier to machine than single crystal SiC [27], the above differences as anticipated, should provide a better surface finish on single crystal SiC compared to polycrystalline SiC. Therefore, SPDT trial in the current work was performed on single crystal SiC (6H-type) in order to measure the attainable surface roughness on this material in a single pass. Since abrasion alone was identified as the cause of tool wear during SPDT of single crystal SiC [28], distilled water (pH value 7) was used as a preferred coolant as it was the one which significantly improved the tribological performance of the diamond during its abrasion with another diamond [29]. In the subsequent sections, the experimental results are presented and discussed.

3. Experimental details

SPDT trial was performed on an ultra precision diamond turning machine (Moore Nanotech 350 UPL). This machine tool has a liquid cooled air bearing spindle having motion error of less than 50 nm while its driving system resolution is upto 0.034 nm [30]. A snapshot of the total experimental assembly is shown in Figure 1.

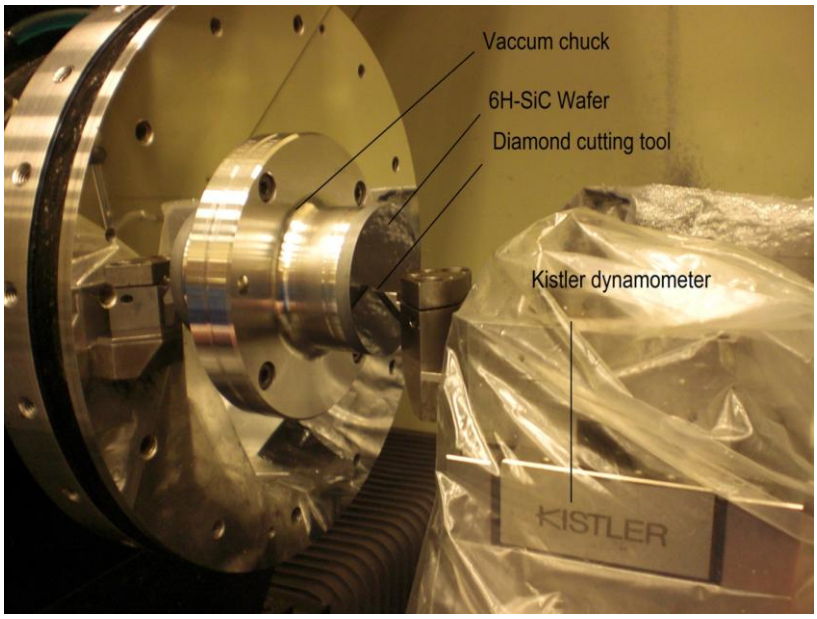

Figure 1: Experimental setup

A three-component force dynamometer unit (Kistler 9257-B) was used for the measurement of the cutting forces. A non-contact measurement of surface roughness was done through a white light interferometer (Zygo NewView 5000) while a form Talysurf surface profilometer was used to measure the surface finish *via* contact measurement. Cutting tool was examined in a high magnification scanning electron microscope (SEM) (FIB- FEI Quanta 3D FEG). The workpiece specimen used was N type-6H-SiC wafer of diameter 50 mm and thickness 5 mm with crystal orientation (001). Conventionally, round nose cutting tools and low feed rates are preferred to obtain a crack free machined surface while machining brittle materials [31]. This experimental study also adopted a round nose cutting tool. Single crystal diamond cutting tool (cubic orientation) having negative rake angle of 25°, 2 mm tool nose radius and 10° clearance angle was used. The machining parameters used in this study were calculated by combining the experimental variables and empirically known relations shown in Table 3.

Table 3: Optimum matrix of machining parameters

S.NO.	Parameters	Unit of measurement	Values
1	Tool nose radius of diamond tool (R)	µm	2000
2	Cutting edge radius of diamond tool	nm	57.4

3	Diameter of workpiece (D)	mm	50
4	Cutting speed (V)	m/sec	1
4	Maximum Feed Rate $f_{\max} = d_c \times \sqrt{\frac{R}{2 \times (d_c + y_c)}}$ Note: Value of d_c and y_c are taken from table 1.	(µm/rev)	0.61 ~ say 0.65
5	Maximum critical depth of cut for 6H-SiC (d)	nm	70 [25]
6	Spindle speed $N = \frac{1000 \times V}{\pi D}$	RPM	382
7	Maximum critical chip thickness When $f < \sqrt{2Rd - d^2}$, where R>>f, R>>d and R is in mm. $t_{\max} = f\sqrt{\frac{2d}{R}}$ [22]	nm	5.438
8	Coolant	pH value 7	Distilled water

4. Experimental observations

4.1. Brittle –Ductile Transition, chip formation and cutting forces

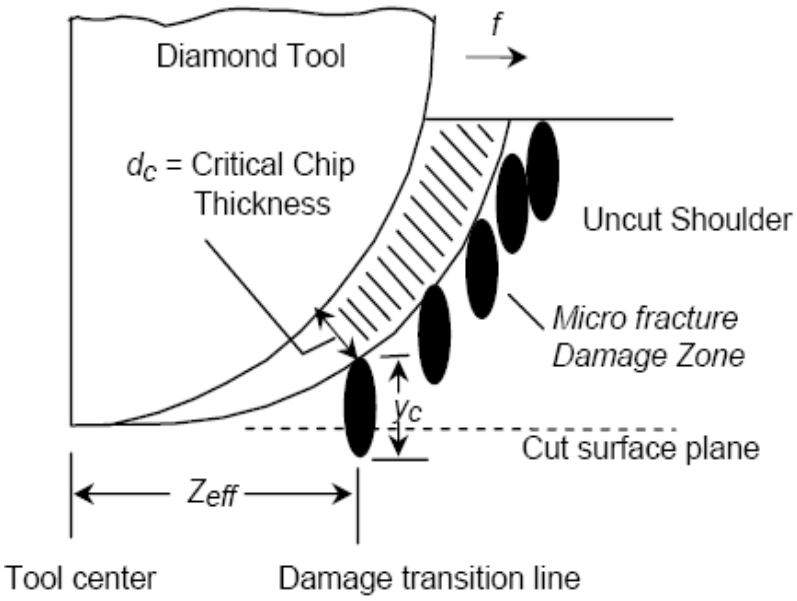

Figure 2: Ductile-regime machining model [18].

Figure 2 shows a cross sectional image of the ductile-regime machining model. Since proposed, this machining model is being used to demonstrate the machining mechanism of all the brittle materials.

During SPDT, the undesirable fracture damage is assumed to originate at the critical chip thickness (d_c) which propagates to a depth y_c. As long as the fracture damage does not penetrate underneath the finished machined surface, ductile regime machining could be executed consistently. The fact to be noticed here is that in the remaining region of uncut shoulder, even if the fracture damage occurs, the fractured material is carried away by the tool in the subsequent cuts. This phenomenon highlights the fact that the materials possessing short critical crack length are more amenable to SPDT.

In the current work, a DXR Raman microscope developed by Thermo Scientific Limited was used to obtain an image shown in figure 3 from an uncut shoulder of 6H-SiC. Figure 3 clearly shows the occurrence of brittle-ductile transition and the associated experimental measurements in accordance with the ductile-regime machining model. Similar to other class of brittle materials such as silicon and germanium, the occurrence of brittle-ductile transition was thus found to occur in 6H-SiC as well which explains the root of the ductility offered by 6H-SiC during the SPDT operation.

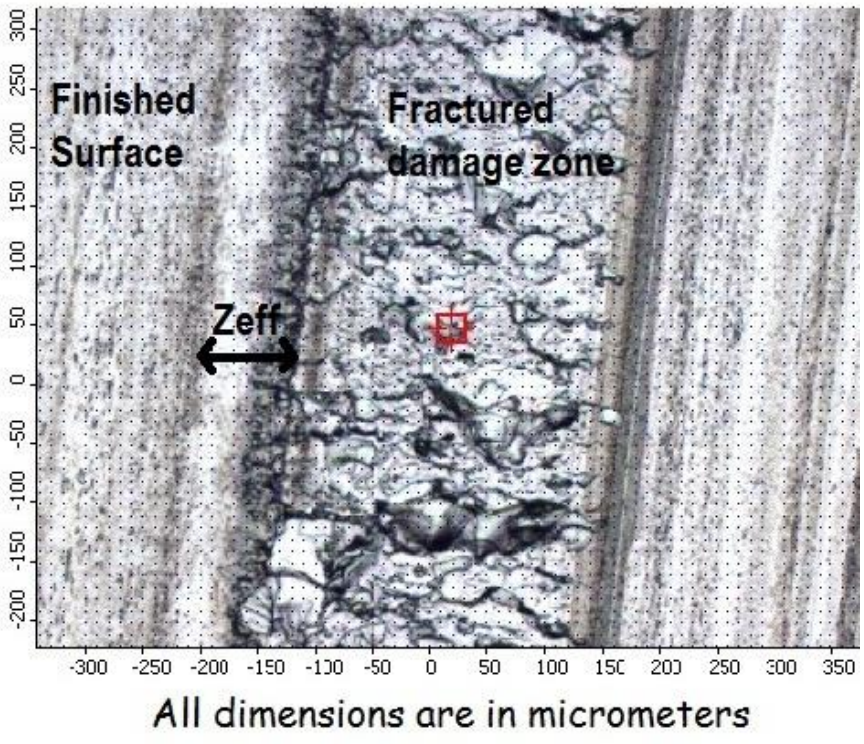

Figure 3: Measured uncut shoulder of diamond turned 6H-SiC using a DXR Raman microscope.

An interesting fact to be noticed is that the critical depth of cut d_c for 6H-SiC is only 70 nm [25] in contrast to the critical depth of cut of another polytype of SiC e.g. 4H-SiC where d_c was obtained as

820 nm [32]. This observation suggests that the material removal rate (MRR) under the same ductile-regime machining conditions would be significantly higher in 4H-SiC in comparison to 6H-SiC. However, a trade off between the quality of finished surface, sub-surface deformation lattice layer depth, tool wear and machining efficiency would dictate a choice of selection between these two polytypes of SiC [21].

On the other hand, polycrystalline SiC has been found more machinable compared to a single crystal SiC on account of the ease of chip formation mechanism as shown in details in figure 7 obtained by molecular dynamics simulation [27]. Figure 4 is a comparison of chip morphology between machining a single crystal SiC and a polycrystalline SiC. As evident from figure 4, the absence of grain boundaries causes tremendous lattice distortion which is responsible for structural transformation of the cutting chips of single crystal SiC [33].

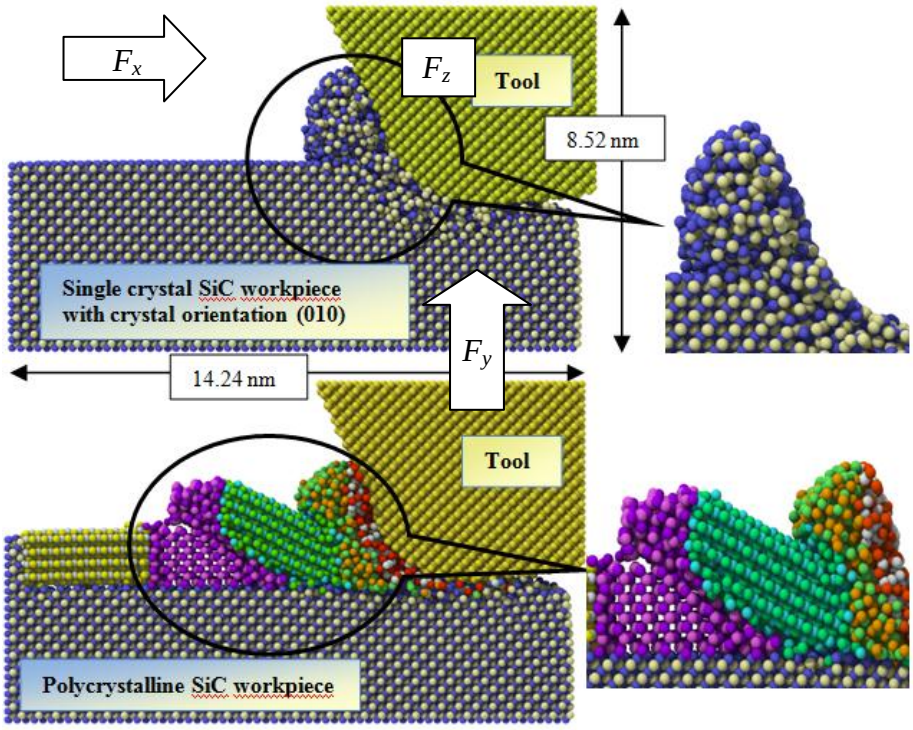

Figure 4: Difference in chip formation mechanism between single crystal and poly-crystal SiC [27].

Such phase transformations are however, obstructed by the presence of grain boundaries during machining of polycrystalline workpiece such as RB-SiC. In an RB-SiC workpiece, the grains of SiC are oriented in different crystal orientations. Thus, some of the grains boundaries cause the individual grains to slide along the easy cleavage direction. This causes the built up of stresses at

the grain boundaries. Consequently, the cutting chips in RB-SiC are not deformed by plastic deformation alone rather a combination of the phase transformation at the grain boundaries and slip of the large size grains both precede in tandem. This is the reason that while silicon bonds underwent amorphization, no phase transformation of 6H-SiC grains was observed while RB-SiC was diamond turned [22]. Since, the cleavage of 6H-SiC grains could occur in random fashion, this mechanism of chip formation explains the observation of high machined surface roughness on RB-SiC compared to single crystal SiC.

The former part of figure 4 also shows schematically the orientation of the components of cutting force acting on the cutting tool during a cutting operation. The "tangential cutting force" (F_x) acts in the x direction, the "thrust force" (F_y) acts in the y direction and F_z acts in the direction orthogonal to the X and Y planes. The evolution of these cutting forces over the period of 2 seconds is presented in figure 5.

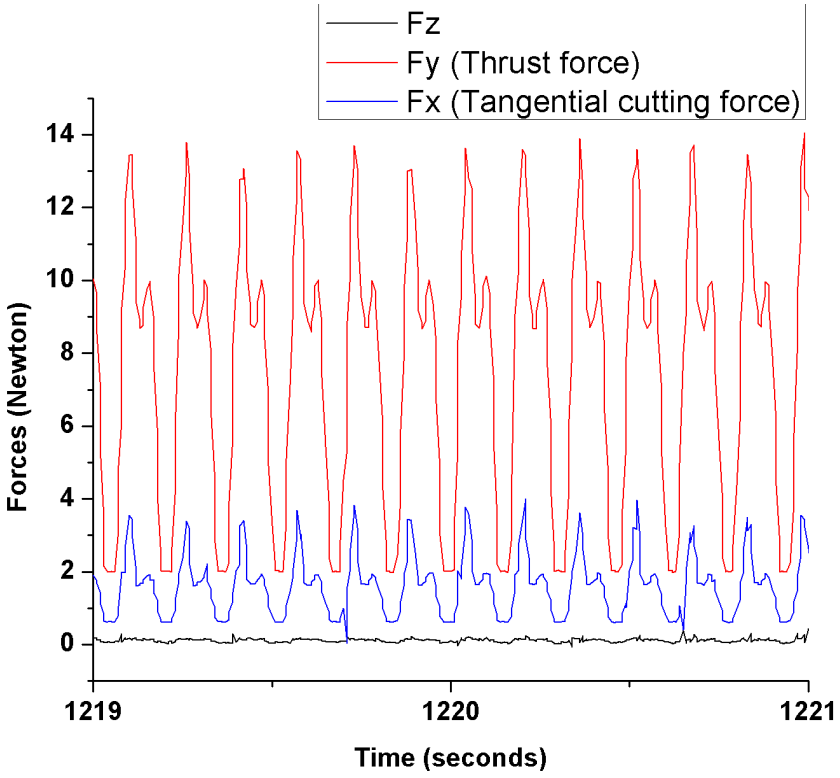

Figure 5: Experimental measurement of cutting forces during SPDT of single crystal 6H-SiC

It is evident from figure 5 that the thrust forces were almost 4 times higher in magnitude than the tangential cutting forces. This could be attributed to the use of high negative tool rake angle which

is central to any SPDT operation. A negative rake causes an increase in the thrust forces [34-35] in contrast to the conventional macro-scale machining where positive rake angle tools are normally used. It is of interest to note that an MD simulation study reported that the dominance of thrust forces over cutting forces during nanometric cutting of silicon is a necessary requirement to execute ductile-regime machining conditions [36]. While this looks in accordance with the current experimental trial on single crystal 6H-SiC, this is not the case observed in similar nanoscale friction based studies where cutting forces were found dominant than thrust forces [21, 37]. Therefore, this is an area of investigation yet to be researched. Furthermore, in contrast to machining silicon [38], both tangential cutting forces and thrust forces during SPDT of 6H-SiC were found almost two and half times larger, suggesting that the cutting resistance of 6H-SiC is significantly higher than silicon [21].

4.2. *Surface roughness*

Figure 6 shows the experimental measurement of machined surface roughness on 6H-SiC during first kilometre of cutting length. The Ra value obtained through Form Talysurf was found as 9.2 nm while white light interferometer measurement was recorded as 10 nm.

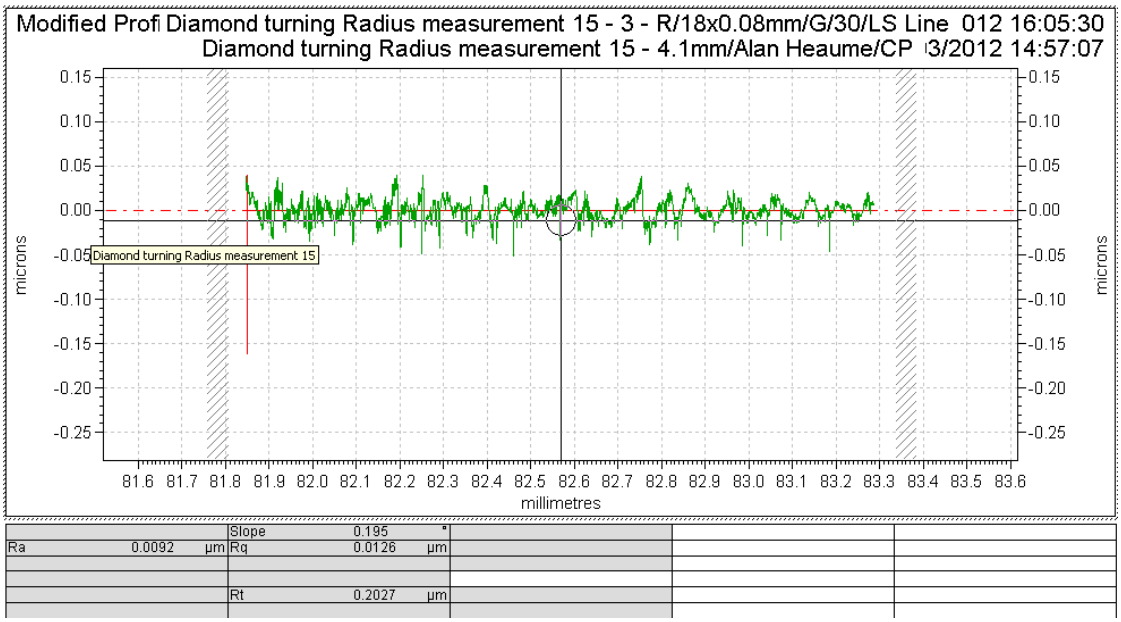

Figure 6: Ra of 9.2 nm measured by Form Talysurf surface profiler after cutting length of one km

Comparing the Ra value obtained in this work with the previously reported Ra values (shown in

Table 1), it confirms the earlier argument that a single crystal SiC provides a better measure of Ra value than polycrystalline SiC [27]. It is also now known that wavelengths in the IR spectral region are longer than those of the visible region, hence, surface roughness specifications are not very stringent for visible components [39]. The surface roughness measurement on 6H-SiC obtained in the current work demonstrates that SPDT is capable to generate a visible optics on SiC directly in a single pass.

4.3. Tool Wear

SiC is known to be chemically inert and therefore the influence of tribochemistry on the wear of diamond tool, unlike machining silicon, becomes negligible [40-41]. However, abrasive wear is apt to occur during the tribological contact of diamond and SiC owing to their ultra high hardness [28]. Figure 7 shows the SEM image of the diamond cutting tool before cutting.

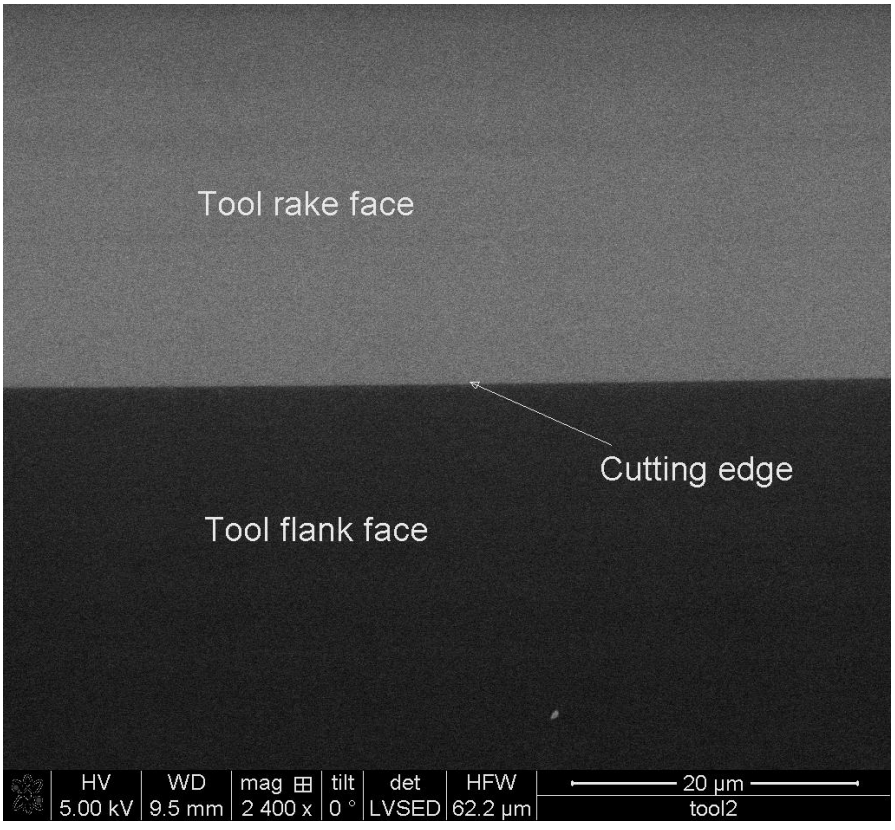

Figure 7: SEM image of the diamond cutting tool before cutting

It can be seen from figure 7 that before cutting, the cutting edge was extremely sharp and both tool flank face and tool rake face were prepared extremely fine without any visible wear marks on the

edge or the surface of the tool. Figure 8 shows the SEM snapshot of the diamond tool on the same magnification after one kilometre of cutting length. It can be seen that cutting tool has started to show wear marks on the flank face and the edge radius has started to lose its sharpness. At some parts recession of the cutting edge is also visible.

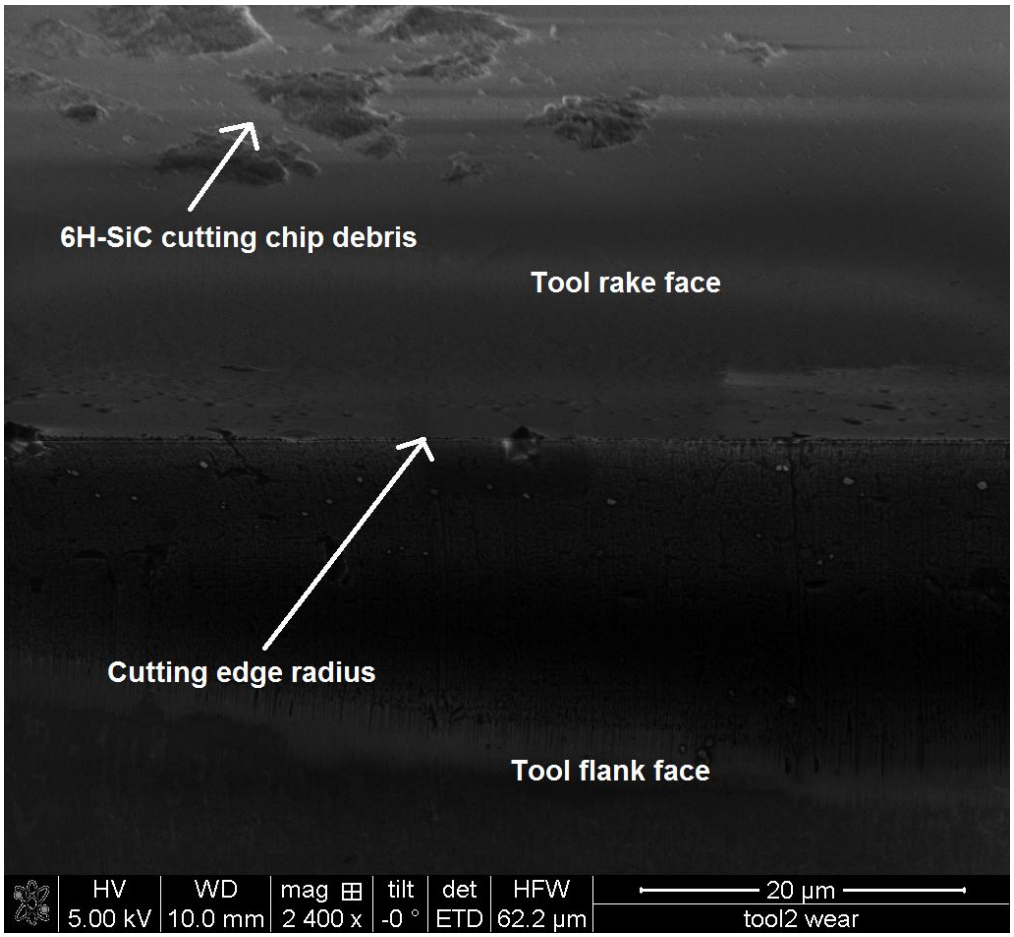

Figure 8: SEM image of the diamond cutting tool after cutting distance of one kilometre.

Besides recession of the cutting edge, significant wear marks on the tool flank face can also be seen. An interesting observation however was that the cutting chips were observed to cling to the tool rake face despite using the liquid coolant. The clinging of cutting chips with the rake face of the cutting tool suggests the existence of ultra high pressure and high flash temperature in the cutting zone during machining of SiC [28, 33]. A recent simulation based study has showed interfacial abrasion to be the dominant mechanism of tool wear during SPDT of SiC which results in graphitization of the diamond [28, 42]. The contribution of distilled water to suppress the tool wear has remained yet another investigation to be performed in future along with a comparison with other coolants

especially copper nanoparticles [23] which were found to provide superior performance while machining RB-SiC.

5. Conclusions

Over the past decade, the proliferation of single point diamond turning (SPDT) investigations has enabled to generate optical finished surfaces on various categories of brittle materials. SPDT of 6H-SiC in the current work is yet another benchmark to this sequence. This study in its current format provides an impetus to understand the microscopic insights of brittle-ductile transition during SPDT of single crystal silicon carbide. The following conclusions are made based on the discussions made in the earlier sections:

1. Single crystal 6H-SiC was diamond turned using a specific coolant of distilled water with pH value of 7. A surface roughness of Ra value 9.2 nm was obtained making SPDT as a feasible option to generate visible range optics on single crystal SiC in a single pass without recourse to any secondary finishing technique such as polishing process.
2. The chip formation mechanism in the case of single crystal SiC and polycrystalline SiC (RB-SiC) is significantly different. While it has been realized over the past decade that structural transformation of brittle materials are responsible for their ductile response or ductile regime machining, this is not the case with RB-SiC. It has been shown that RB-SiC, unlike single crystal SiC involved a different mechanism of chip formation and hence phase transformation of 6H-SiC grains was not found evident in the previous experimental work.
3. The microscopic mechanism for material removal in single crystal SiC involves ductile deformation and brittle fracture, in accordance with the ductile-regime machining model proposed long back in the year 1990. The material removal behaviour seems to be influenced by the type of coolant used which provided an improved machined surface roughness in the current investigation.

4. The occurrence of brittle-ductile transition was captured through the state-of-art DXR Raman microscope. The cutting forces during SPDT of 6H-SiC were found to be on very higher side. They were almost 2 and half times the magnitude of cutting forces while machining single crystal silicon, signifying tremendous cutting resistance of SiC than silicon. Thrust forces were almost four times the cutting forces which are attributed to the use of high negative tool rake angle.
5. Significant wear marks on tool cutting edge and clinging of the cutting chips/debris despite the usage of liquid coolant was observed which impedes the consistent execution of ductile-regime machining operation on a large size silicon carbide workpiece.

Acknowledgements:

The authors would like to thank Mr. Alan Heaume (Cranfield University) and Dr. Jining Sun (Heriot-Watt University) for their experimental assistance. Helpful suggestions of Dr. John Patten (Western Michigan University, USA) and Dr. Jiwang Yan (Kieo University, Japan) are sincerely appreciated. This work is a part of PhD project which was funded through Scottish Overseas Research Students Award (with additional funding from the Neilson fund) from the School of Engineering and Physical Sciences of Heriot-Watt University to which the first author (SG) is always indebted.

References:

1. Neudeck, P.G., *SiC Technology*, in *The VLSI Handbook*, B. Raton, Editor. 2000, CRC Press and IEEE Press: Florida. p. 6.1-6.24.
2. Dzurak, A., *Quantum computing: Diamond and silicon converge.* Nature, 2011. **479**(7371): p. 47-48.
3. Shore, P., et al., *Precision engineering for astronomy and gravity science.* CIRP Annals - Manufacturing Technology, 2010. **59**(2): p. 694-716.
4. John A. Patten, et al., *Chapter 2: Numerical simulations and cutting experiments on single point diamond machining of semiconductors and ceramics*, in *Semiconductor Machining at the Micro-Nano Scale*, J. Yan and J.A. Patten, Editors. 2007, Transworld Research Network: Trivandrum-695 023, Kerala, India.
5. Ravindra, D. and J.A. Patten, *Chapter 4: Ductile regime material removal of silicon carbide(SiC)*, in *Silicon Carbide: New Materials, Production methods and application*, S.H. Vanger, Editor. 2011, Nova Publishers: Trivandrum, India. p. 141-167.
6. Rhorer, R.L. and C.J. Evans, *Fabrication of optics by diamond turning*, in *Handbook of*

Optics. 2010, Mcgraw Hill.
7. Saito, T.T., *Machining of optics: an introduction.* Appl. Opt., 1975. **14**(8): p. 1773-1776.
8. BRINKSMEIER, E., *Micro-Machining*, in *Scientific Discussion Meeting Ultra-Precision Engineering - from Physics to Manufacture*. 2011, Royal Society: London.
9. Patten, J., W. Gao, and K. Yasuto, *Ductile Regime Nanomachining of Single-Crystal Silicon Carbide.* Journal of Manufacturing Science and Engineering, 2005. **127**(3): p. 522-532.
10. Ravindra, D. and J. Patten, *Improving the Surface Roughness of a CVD Coated Silicon Carbide Disk by Performing Ductile Regime Single Point Diamond Turning.* ASME Conference Proceedings, 2008. **2008**(48517): p. 155-161.
11. King, R.F. and D. Tabor, *The Strength Properties and Frictional Behavior of Brittle Solids*, in *Series A: Mathematical and Physical Science*. 1954, Proceedings of the Royal Society of London. p. 225-238.
12. Bridgman, P.W. and I. Simon, *Effects of Very High Pressures on Glass.* Journal of Applied Physics, 1953. **24**(4): p. 405-413.
13. Lawn, B. and R. Wilshaw, *Indentation fracture: principles and applications.* Journal of Materials Science, 1975. **10**(6): p. 1049-1081.
14. Niihara, K., *Slip systems and plastic deformation of silicon carbide single crystals at high temperatures.* Journal of the Less Common Metals, 1979. **65**(1): p. 155-166.
15. Lawn, B.R. and D.B. Marshall, *Hardness, Toughness, and Brittleness: An Indentation Analysis.* Journal of the American Ceramic Society, 1979. **62**(7-8): p. 347-350.
16. Marshall, D.B. and L. B.R., *Indentation of Brittle Materials*. Microindentation Technology in Materials Science and Engineering. Vol. 889. 1986: ASTM STP,.
17. Bifano, Dow, and Scattergood, *Ductile-Regime Grinding: A New Technology for Machining Brittle Materials.* Journal of Engineering for Industry, 1991. **113**(184).
18. Scattergood, R.O., Blake, N., *Ductile-regime machining of germanium and silicon.* Journal of the American ceramic society, 1990. **73**(4): p. 949-957.
19. Patten, J.A., *High Pressure Phase Transformation Analysis and Molecular Dynamics Simulations of Single Point Diamond Turning of Germanium,*, in *Mechanical*. 1996, North Carolina State University: Raleigh N.C.
20. Ravindra, D., *Ductile mode material removal of ceramics and semiconductors*, in *Department of Mechanical and Aeronautical Engineering*. 2011, Western Michigan University: Michigan. p. 312.
21. Luo, X., S. Goel, and R.L. Reuben, *A quantitative assessment of nanometric machinability of major polytypes of single crystal silicon carbide.* Journal of the European Ceramic Society, 2012. **32**(12): p. 3423-3434.
22. Yan, J., Z. Zhang, and T. Kuriyagawa, *Mechanism for material removal in diamond turning of reaction-bonded silicon carbide.* International Journal of Machine Tools and Manufacture, 2009. **49**(5): p. 366-374.
23. Yan, J., Z. Zhang, and T. Kuriyagawa, *Effect of Nanoparticle Lubrication in Diamond Turning of Reaction-Bonded SiC.* International Journal of Automation Technology, 2011. **5**(3): p. 307-312.
24. Patten, J. and J. Jacob, *Comparison between numerical simulations and experiments for single-point diamond turning of single-crystal silicon carbide.* Journal of Manufacturing Processes, 2008. **10**: p. 28-33.
25. Jacob, J., et al., *determination of the ductile to brittle transition and critical depth of cut in 6h-silicon carbide through fly cutting*, ed. P. NO.1748. 2005: ASPE.
26. Shayan, A.R., et al., *Force Analysis, Mechanical Energy and Laser Heating Evaluation of Scratch Tests on Silicon Carbide (4H-SiC) in Micro-Laser Assisted Machining ([micro sign]-LAM) Process.* ASME Conference Proceedings, 2009. **2009**(43611): p. 827-832.
27. Goel, S., et al. *Influence of nanoparticle coolant and crystal structure of the workpiece during nanometric cutting of silicon carbide*. in *P6.75- Proceedings of the 12th EUSPEN International Conference, Volume 2, Page 299-302*. 2012. Stockholm: EUSPEN.

28. Goel, S., et al., *Atomistic aspects of ductile responses of cubic silicon carbide during nanometric cutting.* Nanoscale Research Letters, 2011. **6**(1): p. 589.
29. Grillo, S.E. and J.E. Field, *The friction of natural and CVD diamond.* Wear, 2003. **254**(10): p. 945-949.
30. Luo, X., *High Precision Surfaces Generation: Modelling, Simulation and Machining Verification*, in *Mechanical Engineering*. 2003, Leeds Metropolitan University: Leeds.
31. Yan, J., Syoji, Katsuo, Kuriyagawa, Tsunemoto, Suzuki, Hirofumi, *Ductile regime turning at large tool feed.* Journal of Materials Processing Technology, 2002. **121**(2-3): p. 363-372.
32. Ravindra, D. and P. J.A., *Determining the Ductile to Brittle Transition (DBT) of a Single-Crystal 4H-SiC Wafer by Performing Nanometric Cutting*, in *ISAAT 2007 Precision Grinding and Abrasive Technology at SME International Grinding Conference*. 2007.
33. Goel, S., X. Luo, and R.L. Reuben, *Shear instability of nanocrystalline silicon carbide during nanometric cutting.* Applied Physics Letters, 2012. **100**(23): p. 231902.
34. Fang, F.Z. and V.C. Venkatesh, *Diamond Cutting of Silicon with Nanometric Finish.* CIRP Annals - Manufacturing Technology, 1998. **47**(1): p. 45-49.
35. Patten, J.A. and W. Gao, *Extreme negative rake angle technique for single point diamond nano-cutting of silicon.* Precision Engineering, 2001. **25**(2): p. 165-167.
36. Cai, M.B., X.P. Li, and M. Rahman, *Study of the mechanism of nanoscale ductile mode cutting of silicon using molecular dynamics simulation.* International Journal of Machine Tools and Manufacture, 2007. **47**(1): p. 75-80.
37. Zykova-Timan, T., D. Ceresoli, and E. Tosatti, *Peak effect versus skating in high-temperature nanofriction.* Nature Materials, 2007. **6**(3): p. 230-234.
38. Durazo-Cardenas, I., et al., *3D characterisation of tool wear whilst diamond turning silicon.* Wear, 2007. **262**(3-4): p. 340-349.
39. RIEDL, M., *Advances in single-point diamond turning provide improved performance for visible as well as IR optics.*, SPIE Magazine by Precitech (July 2004). p. 26-29.
40. Goel, S., et al., *Influence of temperature and crystal orientation on tool wear during single point diamond turning of silicon.* Wear, 2012. **284–285**(0): p. 65-72.
41. Goel, S., X. Luo, and R.L. Reuben, *Wear mechanism of diamond tools during single point diamond turning of Silicon (in press).* Tribology International, 2012.
42. Goel, S., X. Luo, and R.L. Reuben, *Molecular dynamics simulation model for the quantitative assessment of tool wear during single point diamond turning of cubic silicon carbide.* Computational Materials Science, 2012. **51**(1): p. 402-408.

Brittle ductile transition during diamond turning of single crystal silicon carbide

Goel, Saurav

2013-02-28T00:00:00Z